Vol 8 | Issue 1 | Pages 636-649

Journal of Aerospace Engineering and Mechanics

ISSN: 2578-6350

Research Article

DOI: 10.36959/422/469

E-Beam and Solar Thermal Driven Oxygen and Metal Production from Lunar Regolith

Robert W. Moses[1], Sang H. Choi[2], Cheol Park[2] and Catharine C. Fay[2]*

[1]*Retired Senior Engineer, NASA Langley Research Center, Hampton, Virginia, USA*

[2]*Senior Scientists, NASA Langley Research Center, Hampton, Virginia, USA*

Abstract

NASA envisions commercial operations will start with production of tens of metric tons of oxygen per year but will evolve into hundreds to thousands of metric tons of a variety of commodities including oxygen, water, propellants, construction, and manufacturing feedstock. NASA also envisions that commercial lunar mining and processing systems will adhere to the principles of ethical and responsible use of space, especially those identified in "Moon to Mars Objectives" and "Artemis, Ethics and Society: Synthesis from a Workshop" publications. NASA published in 2021 a system concept that illustrates the separation of oxygen and metals from lunar regolith by combining an electron beam (E-beam) with concentrated sunlight. Herein, that system concept has been analyzed in more detail using the current state of the art in E-beam system technology, known dissociation properties of some materials, and an assumption pertaining to the reactant properties of regolith to electrons as design constraints. Our theoretical analysis shows that the combination of solar thermal, E-beam spectral, and E-beam thermal offers a great advantage to increase the production rates of oxygen and metals from lunar regolith. The electron beam system, when combined with the solar concentrator, offers an ethical and responsible use of space by tapping clean energy while producing no nuclear waste or chemical byproducts.

Keywords

Oxygen and metals extraction from lunar regolith, Electron beam, Solar concentrator, Solar thermal, E-beam thermal, E-beam spectral, Responsible mining, Commercial ISRU (*in situ* resource utilization), Industrial scalable production rate, Oxygen from regolith, Metal from regolith.

Introduction

A major objective of NASA's Space Technology Mission Directorate (STMD) is to enable a sustainable human lunar exploration program through the establishment of lunar infrastructure and commercial space operations. A key aspect in achieving this objective is characterizing the resources that exist on the Moon and Mars and learning how to extract and utilize them responsibly to create products for crew, power, transportation, and infrastructure. *In Situ* Resource Utilization (ISRU) is the ability to make products from local materials and offers the potential to significantly reduce costs, mass, risk, and Earth dependency. To advance this objective, NASA seeks information on potential lunar demonstrations of ISRU oxygen extraction from lunar regolith in pursuit of production, capture, and storage of oxygen on the lunar surface [1,2]. NASA's programmatic aim is to maximize partnerships and provide support for commercial lunar operations. To reduce the risk of implementing commercial ISRU operations, initial lunar demonstrations will need to both obtain critical data on lunar regolith and the environment, as well as demonstrate critical technology performance and operations in the actual lunar environment, especially for technologies that interact with lunar regolith. Demonstrations need to close technology and capability gaps for ISRU to address the NASA ISRU Envisioned Future Priorities [3], and NASA's Moon to Mars Strategy. The primary emphasis of the request for information (RFI) was the Objectives Development objective LI-7 with additional lunar infrastructure (LI) objectives, and Recurring Tenets as secondary objectives [4]. From a technical perspective, a main driver for the first lunar ISRU oxygen extraction demonstration is to obtain information on South Pole lunar regolith and validate aspects of oxygen extraction from regolith. Both will reduce the risk and advance the likelihood of commercial ISRU operations on the lunar surface. NASA envisions that commercial operations will start with production of tens of metric tons of oxygen per year but will evolve into hundreds to thousands of metric tons of oxygen, water, propellants, construction and manufacturing feedstock, and additional commodities. NASA also envisions that commercial lunar

***Corresponding author:** Robert Moses, NASA Langley Research Center, USA

Accepted: November 20, 2024

Published online: November 22, 2024

Citation: Moses RW, Choi SH, Park C, et al. (2024) E-Beam and Solar Thermal Driven Oxygen and Metal Production from Lunar Regolith. J Aerosp Eng Mech 7(1):636-649

mining and processing systems will adhere to the principles of ethical and responsible use of space [5], especially those identified in Moon to Mars Objectives Recurring Tenet - 6 (RT-6), Science Enabling - 7 (SE-7), Operation Goal -12 (OP-12), and Lunar Infrastructure - 8 (LI-8).

Regarding the current state of the art (SOA), various oxygen and metal extraction processes continue to evolve with an emphasis on demonstration missions on the lunar surface. Several of these processes continue to show significant promise according to Schluter and Cowley who describe their general principles, thermodynamic fundamentals, possible reactor layouts, and current state of the art: Extraction via a reactive gas; reduction via electrolysis; vapor phase pyrolysis; and thermal extraction of volatiles and water ice [6]. Hydrogen reduction of ilmenite ($FeTiO_3$), methane (CH_4) reduction of ilmenite and fluorination reduction with electrolysis, molten regolith electrolysis and molten salt electrolysis, vapor phase pyrolysis, carbothermal reduction, chemical beneficiation or plasma processing of regolith are at various levels of research and development and are generally regarded as laboratory proven methods [7]. The hydrogen reduction, carbothermal reduction, molten regolith electrolysis and molten salt electrolysis known for lunar oxygen production are in early stages of development, specifically considering for lunar operation that requires respectively a front- and a rear-end systems for feeding process of raw materials and for sorting and placing the processed products into individual component and in storage [8].

Regardless of the significant promise shown during terrestrial and ground-based testing under some simulated lunar conditions, any process must be tailored to anticipate operations on the lunar surface. Expectations are that the processes that have functional parts and design features that are adaptable to the lunar surface environment and other mission constraints have the greater chance of economic viability as well as long-term sustainability. Shaw, et al., suggest that current mineral processing and metal extraction technologies are not adequately equipped to address the extremely harsh lunar environment [9]. In their review of the metals available for extraction, the conditions at the lunar surface, and an analysis of the challenges associated with comminution, beneficiation, and metal extraction operations, they suggest that elimination of traditional comminution and beneficiation stages and their replacement with basic classification could be economically favorable. They conclude that the most promising metal reduction pathways are identified as molten regolith electrolysis, and vacuum thermal dissociation, other processes with merit are hydrogen reduction, carbothermal reduction, and solid electrolysis. However, as they illustrate, each of these pathways face considerable challenges when scored against key lunar environmental factors: gravity; average surface temperature; pressure; human access; day/night cycle; water availability; and dust. The lunar environmental factors and their impacts on processing are summarized in Table 1.

Shaw, et al., states that the primary concerns in the evaluation of metal reduction processes for use on the Moon are reagent usage and supply chain costs, energy requirements, feedstock availability, and process complexity [9]. They analyzed the potential of each process based on the above-mentioned concerns and provided a generalized usability assessment of the possible metal extraction techniques for lunar use to date. Their assessment cited the research target resource, the useful byproducts, condition requirements (elevated operational temperatures mostly), reagents/required wear parts, and an overall assessment, which are summarized in Table 2.

Table 1: Comparison of the environmental effects of the Earth versus Moon on processing, adapted from Shaw, et al. [9].

Factor	Impact
Gravity, 1.62 m/s^2	Impacts density separations; Reduces gravity-driven fluid/particle flow; Increases influence of non-gravity motive forces (surface tension, magnetic attraction etc.); Decreases head pressure, increasing potential pumping heights.
Average surface temperature, 123 °C (Day) - 178 °C (Night)	Temperature variation will affect particle properties e.g. Equipment must be able to survive extreme thermal variations.
Pressure, Unmeasured (Day) 3×10^{-15} atm (Night)	Fluids must be used in a closed system with artificial pressure; Reduction in energy requirements for dissociation; Convective cooling not an option outside of closed systems.
Human Access, Severely restricted	Highly reliable equipment (uncommon in terrestrial mining and metallurgy) is necessary. Modular designs will facilitate repairs/replacements. Autonomously controlled and automated robotic or remotely controlled uncrewed equipment preferable.
Day/Night Cycle, 708.7 hours	Regolith becomes less charged at night (no UV charging). Equipment cooling/ heating is power intensive. Power generation at night becomes challenging, requires large power storage for solar based power solutions.
Availability of Water and other process-required resources, Rare	Geochemical effects on feed material. Comminution and beneficiation processes need to be designed without the use of water. Renders the majority of terrestrial technologies useless.
Dust, Electrostatic, abrasive, and everywhere	Dust suppression and/or mitigation technologies will become essential.

Table 2: Possible metal extraction techniques for lunar use adapted from Shaw, et al. [9].

Process	Reagents and Required wear parts	Overall assessment
Carbothermal Reduction	Carbon (Solid, Methane, CO)	Medium process complexity, regents required, requires artificial atmosphere
Hydrogen Reduction of Ilmenite	Hydrogen	Medium process complexity, regents required, requires artificial atmosphere, limited feedstock availability
Molten Oxide Electrolysis (MOE)	Electrolyte ($CaCl_2$ - CaO, or SiO_2 - B_2O_3 - Na_2O, LiF, CaF_2, MgF_2, Na_2O, $NaBO_4$, Na_3PO_4, $Na_5P_3O_{10}$, NaF - AlF_3) Anodes	Medium process complexity, regents required, requires partial artificial atmosphere, high electrical load
Molten Regolith Electrolysis (MRE)	Anodes	Medium process complexity, electrodes required, requires partial artificial atmosphere, high electrical load
Solid Electrolysis	Electrolyte ($CaCl_2$ - CaO, AlF_3) Anodes	Medium process complexity, regents required, requires partial artificial atmosphere, lower electrical load
Thermal Decomposition	Hydrogen	Medium process complexity, no regents required, low electrical load (requires access to sunlight)
Ionic Liquid & Aqueous Electrolysis	Ionic Liquids, Water, Electrodes, Sulfuric acid or Phosphoric acid in some cases.	High process complexity, regents required, requires artificial atmosphere, medium electrical load
Aluminothermic Reduction	Conducted in electrolyte (NaF, AlF) Anode ($Fe_{0.58}Ni_{0.42}$) Initial reactant (Al)	High process complexity, regents required, requires partial artificial atmosphere, high electrical load
Lithium Reduction	Electrodes ($FeSi_2Li_x$, Pt, $La0.89Sr0.1MnO_3$), Reactant (LiF, LiCl or Li_2O), Electrolyte (ZrO_2), Catholyte ($La_{0.89}Sr_{0.1}MnO_3$)	High process complexity, regents required, requires partial artificial atmosphere, high electrical load
Acid Reduction	HF, H_2SO_4	High process complexity, regents required, requires artificial atmosphere, limited feedstock availability
Fluorine Reduction	KF, LiF, NaF, or HF	High process complexity, regents required, requires partial artificial atmosphere, high electrical load
Bio-Reduction	Bacteria, Water, Defined Minimal Medium	High process complexity, regents required, requires artificial atmosphere, needs high precision temperature control
Carbochlorination	Cl (g), Carbon (s), Hydrogen and/or water	High process complexity, regents required, requires partial artificial atmosphere, medium electrical load, specific feedstock required
Calcium Reduction	Molten Salt ($CaO/CaCl_2$) Electrodes Initial reactant (Ca)	High process complexity, regents required, requires partial artificial atmosphere, high electrical load

Our technical approach for combining solar with e-beam is that the regolith will be heated and e-beamed to remove the oxygen at temperatures below the melting points so that the oxygen is separated from the regolith and from the oxides so that the remaining solids are metals that fall towards the lunar surface by lunar gravity. E-beam energy breaks the chemical chain of oxides. Afterwards, oxygen atom flies away. The metal part may remain at the same location or relocated. The excessive energy of electron might heat regolith up at the same time, but it takes time to melt regolith because of time constant (specific heat of regolith). E-beam spectral is instantaneous. Hence, the regolith will be heated prior to the melting point(s) of element(s) remaining in the regolith, the oxygen liberated using the e-beam spectral and then extracted from the chamber. Induction heating will be used for processing/separating the metals from each other. The electron beam (E-beam) approach presented here is not limited to a single mineral, is not impacted by reduced gravity, can handle temperature variations, prefers vacuum, can be fully automated, does not require water, and can be isolated from dust. The power and cooling can be accommodated by solar based power solutions, especially near the lunar poles. As will be demonstrated herein, the e-beam approach can be scaled to lunar surface operations to produce tons of oxygen and metals per year.

By further comparison with methods similar to electron beam, Rasera, et al., mentioned that ion bombardment is commonly used in terrestrial beach sands processing for the separation of ilmenite and rutile from quartz [7]. While E-beam technology has not been studied directly for use in ISRU, Agosto (1985) noted that gas ionization likely contributed to the superior performance of his apparatus under air and nitrogen than vacuum [10]. The production and ejection of ions in space is not uncommon; ion thrusters are used regularly for satellite station keeping. Similar technology could be employed for particle charging lunar ISRU processes. Electron beam charging has a lower energy requirement

to produce the beam compared to that required for gas ionization [11]. Additionally, it eliminates the need for an ion source. The charging of granular material under vacuum using ion, electron and ultra-violet (UV) bombardment naturally happens on the lunar surface by impinging protons, electrons, and UV carried by solar flares. The phenomenon was experimentally demonstrated by Wang, et al., (2016) to explain particle transport on airless bodies [12]. In their experiments, silica-rich Martian regolith simulant, composed of 38-48 μm particles, was charged using a combination of ions and electrons, electrons only, and UV exposure. They found that the charge imparted on the samples by the electron beam was an order of magnitude greater than the combined ion/electron bombardment, and three orders of magnitude greater than the UV method.

Another technique called "ablative arc mining" would allow for water, metals and other resources to all be pulled from the lunar surface material all at once, improving upon older lunar mining concepts and methods [13]. The technique would use an arc of electricity and would be "like putting lightning over the surface of the moon". In the technique, arcs of electric current across two electrodes would sublimate frozen water out of the lunar regolith, or surface material, turning it into water vapor. It would also pull other things like metals out of the lunar material. The electric arc would then break apart the water (or other materials like metals) into ionized particles. The main challenge in ablative arc mining is that it takes quite a lot of power to create an electrical arc in the moon's high-vacuum atmosphere. To sustain the electrical arc between electrodes, an intervening medium is necessary as electron hopping stations at the same time to multiply electrons in the arc stream. Otherwise, electrical arc in lunar vacuum requires excessively high discharge voltage. Suppose that fine particles of regolith are instead used between electrodes for arc discharge. The electrode damages by the impact of ionized fine particles of regolith are substantial, so that the replacement of cathode electrode should be done frequently [14]. As described, ablative arc mining sounds similar to arc welding which requires a working gas.

The goal of this paper is to demonstrate theoretically the feasibility compared to and in combination with concentrated sunlight that an electron-beam system can liberate oxygen and metals from lunar regolith. Experimental investigations are planned for validating our analysis and will be presented at a later date. Our analysis herein illustrates the relative production rates from Highlands regolith when using solar thermal, e-beam spectral, and e-beam thermal separately and when combined.

Materials and Methods

NASA published a system concept that illustrates the separation of oxygen and metals from lunar regolith by combining an electron beam with concentrated sunlight [15]. Solar power concentrated by a 10-meter diameter aperture of a Cassegrain system is approximately 85 kW after accounting 20% optical loss. If a certain amount of regolith is set to be processed using a designated power input, the time required can be roughly determined as:

$$\Delta t = \frac{m \cdot c_p \cdot \Delta T}{q_s}$$

Where m is the mass of regolith for processing, c_p the specific heat of regolith, ΔT the temperature to heat, and q_s the solar power. It is known that 60.9% of regolith is oxygen as shown in Figure 1 [16]. The composition of the regolith varies slightly between Highlands or Mare regions. McKay and Williams [17] stated that anorthite ($CaAl_2Si_2O_8$) and ilmenite ($FeTiO_3$) are a suitable feedstock for extracting metals such as aluminum, silicon, titanium, and iron. Anorthite is a combined formation of CaO, Al_2O_3, and $2SiO_2$ while ilmenite with FeO and TiO_2. Based on the samples of Apollo 15, 16, and 17, lunar highland soils contain up to 60% anorthite of which comprises 19% aluminum and 20% silicon. Ilmenite is known be 10% in mare soils that contain 32% titanium and 37% iron [17]. A large portion of regolith mostly contains the extractable metals including silicon, out of the total oxides of regolith. In addition, as shown in Figure 1, the regolith contains pure metals that comprise of 37.42 At % level. Figure 1 also describes the lunar radiation environment, such as solar wind, solar flare, micrometeoroids, and galactic cosmic rays that carry substantial energy and contributes to the dissociation of oxides upon impact. Note that based on future NASA goals, the composition of the regolith on the South pole would be of more interest. In this analysis, an average Highlands composition data is used.

Here the key objective is the extractable rates of oxygen and metals, including other extractable resources such as silicon, from oxides in the regolith. Note that for convenience, silicon is included in the category of metal in this analysis. The extractable rates of oxides are dependent on breakdown methods of oxides. A case study made here is to analyze a new oxide breakdown method that uses a combination of E-beam and solar power together. As described below, the e-beam has both thermal and spectral effects on the breakdown process. We attempt to model herein as separate effects the e-beam thermal contribution and the e-beam spectral contribution. Energetic electrons carrying several tens of kilo-electron volts (keV) level kinetic energy can ablate materials upon contact. We plan to use this process to split the oxide molecules instantaneously from the regolith. The energy required to split the oxide molecules is relatively very low (< 10 eV) as listed in Table 3. The energy (30 keV and 60 keV) of E-beam systems considered here for decomposition of lunar oxides is exceedingly high compared to the breakdown energies shown in Table 3. At these high energies, the impinging electrons are expected to continuously breakdown the oxide molecules in a sequence not only of the primary interactions but also in the secondary, the tertiary, or higher order interactions until the electron energy is all consumed. Our analysis attempts to estimate these interactions.

In this case study, the E-beam thermal was also considered for the decomposition of lunar oxide molecules using the 2 or 4 beamlines of 250 mA accelerated by either 30 keV (7.5 kW) and 60 keV (15 kW). By assuming that the energy of these beamlines is all converted into thermal energy, the decomposition of oxide molecules was

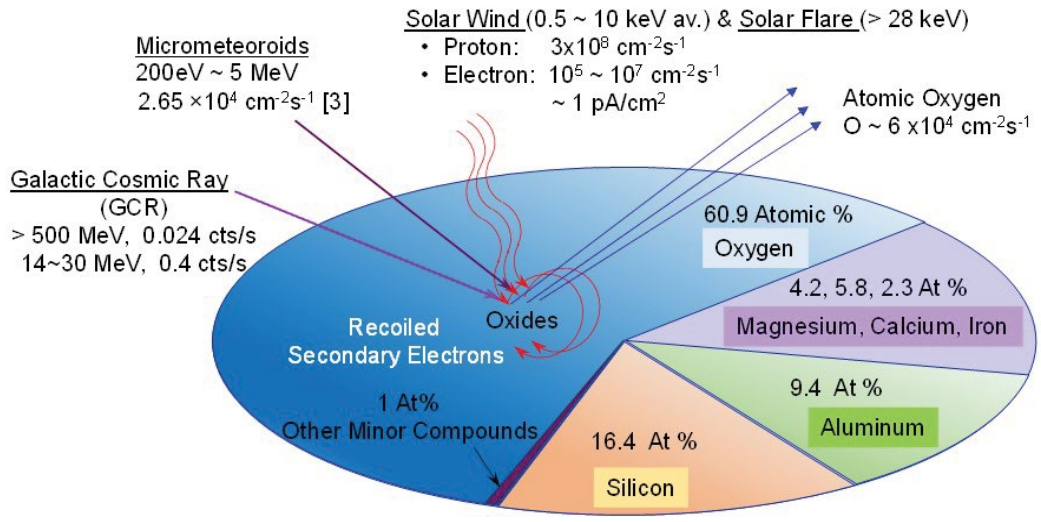

Figure 1: Composition of average Mare lunar regolith under lunar environment, adapted from Turkevich [16] and Cremonese [18].

Table 3: Composition and dissociation energy of oxides in highlands regolith. Turkevich [16], Ptacek [19], Brewer [20], Lide [21], and McKay [17].

Oxide	Oxide in reolith [13]	Dissociation Energy [14,15]			Gram Mol			Gram Mol Ratio		Molar % in Oxide	
					m_{Mol}	O_2	Metal	O_2	Metal	O_2	Metal
	%	KJ/mol	eV	J/g	g mol	G mol	g mol	%	%	g mol	g mol
SiO_2	45.5	707.6	7.33	11793	60	**32**	**28**	53	47	**14.56**	**12.74**
Al_2O_3	22.2	1030	10.67	10098	102	**48**	**54**	47	53	**10.66**	**11.99**
FeO	7.5	410.3	4.25	5699	72	**16**	**56**	22	78	**1.2**	**4.2**
CaO	15	431.3	4.47	7702	56	**16**	**40**	28	72	**2.4**	**6**
MgO	7.8	418.7	4.34	10468	40	**16**	**24**	4	6	**1.25**	**1.87**
TiO_2	1.3	669.9	6.94	8374	80	**32**	**48**	4	6	**0.42**	**0.62**
Anorthite	60% [17]	1165 [19]	12.07	4191	278	128	150	46	54	76.8	90
Ilmenite	10% [17]	1154	11.9	7592	152	48	104	32	68	4.8	10.4

estimated and compared with the E-beam spectral cases. In the decomposition process, only 30.49g mol of regolith has extractable oxygen and 37.42g mol of regolith is extractable metals as shown in Table 3. The molar weight of oxygen and metal from each oxide are listed in the 7th and 8th columns of Table 3. For example, silicon dioxide (SiO_2) that comprises of 45.5% has 32 gram mol of oxygen and 28 gram mol of silicon. The actual molar weights of oxygen and silicon available in regolith are 14.56 g mol and 12.74 g mol molar weight, respectively.

NASA's system concept has been analyzed in more detail using the current SOA in E-beam system technology and known dissociation properties of some materials as design constraints. Based on assumptions for dissociation properties and processing methods of lunar regolith and ilmenite [9,22,23], our analysis indicates that multiple E-beam guns are required to extract oxygen and metals from regolith.

However, existing E-beam systems are much heavier and larger than required for lunar surface operations due to the fact that terrestrial systems include a pressure vessel to provide a vacuum while operating in atmospheric pressure on Earth. On the Moon, the vacuum is provided naturally with 10-12 Torr. Taking this natural vacuum condition into account will allow huge reductions in the E-beam system mass and volume for use on the Moon compared to terrestrial systems. In the E-beam interaction, two dominant coupling modes comprise the dissociation of lunar regolith oxides. Direct-coupling to split oxide molecules with an electron energy higher than the binding energy of oxide molecules is regarded as E-beam spectral. Indirect coupling is regarded as thermal that is caused by an unstable resonant mode of atomic or molecular oscillation by loaded E-beam energy.

E-beam Spectral

The E-beam guns considered for this demonstration are the units that emit 250 mA level current of electrons which is equivalent to 1.5625×10^{18} electrons with 30 keV and 60 keV energy, respectively. The E-beam spectral is based on the fact that energetic electrons (30 keV or 60 keV) couple directly with and dissociate oxide molecules into oxygen and metal using a portion of their energy in collision. Those electrons with energy, like Compton electrons, dissipate energy through

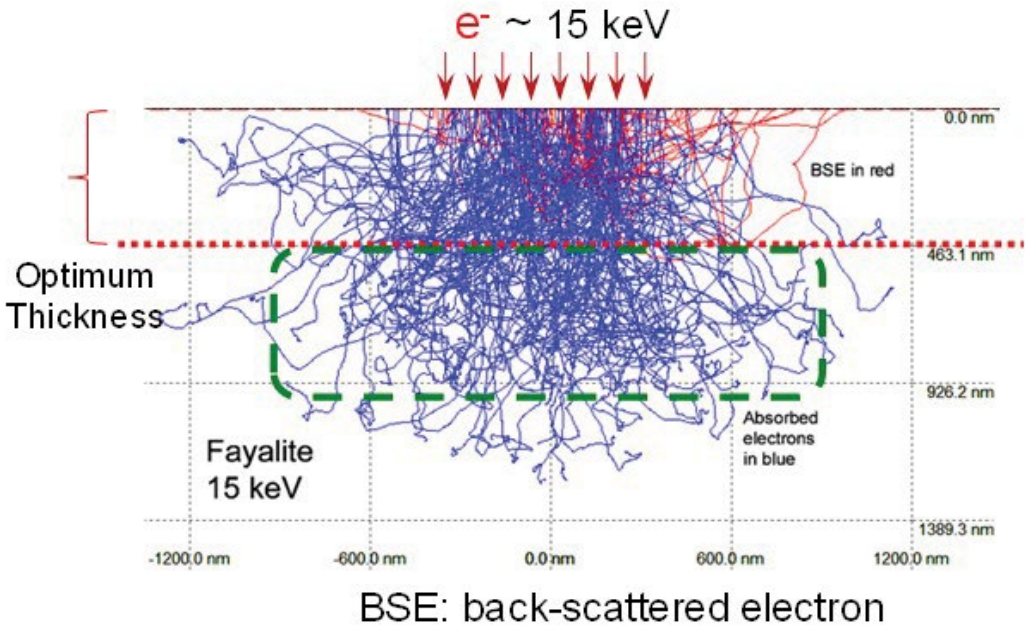

Figure 2: Monte Carlo analysis of 15 keV electron penetration into fayalite material [24].

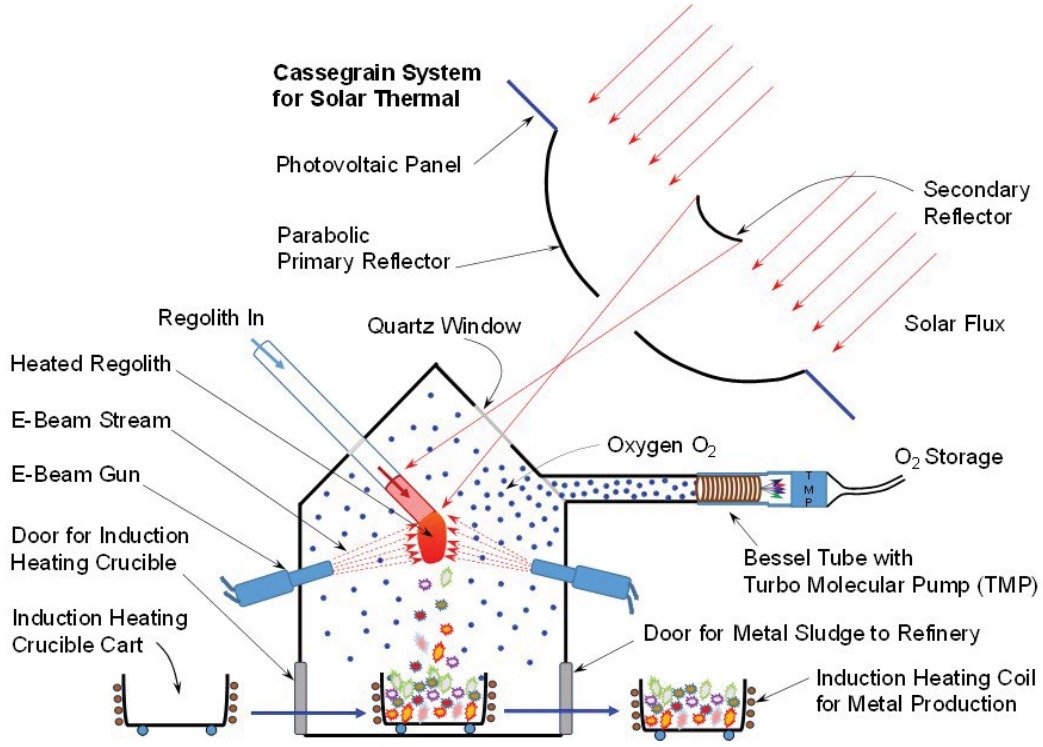

Figure 3: System concept for decomposition of oxides in lunar regolith using solar thermal, solar spectrum, and electron beam.

collisions until their kinetic energy is diminished by primary, secondary, tertiary, and additional high-order collisions. The penetration depth or mean-free-path of energetic electrons depends on electron energy and the density of materials. The number of electrons engaged in collisions with oxide molecules with their energy greater than the binding energy of oxide molecules potentially contributes to the direct split of oxides into oxygen and metal (Figure 2).

E-beam Thermal

The collisional energy often causes an unstable resonant mode of atomic or molecular oscillation without splitting oxides dissipating the energy of electrons as a thermal mode. In this case when E-beam thermal is assumed to dominate the interaction, the thermal contribution of four E-beam units (15 kW/unit) is 60 kW. If E-beam thermal is simply added to

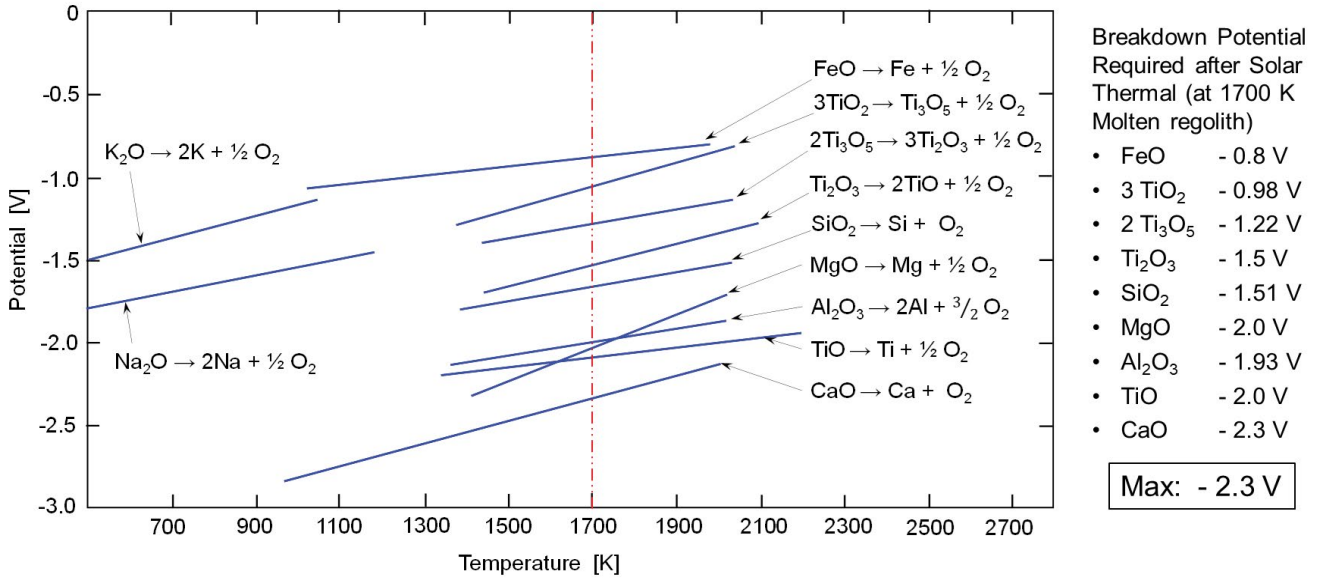

Figure 4: Dissociation energy requirement of oxides along with temperature [6].

solar thermal from the Cassegrain solar concentrator, the production rates by thermal processing increase substantially, as described in Figure 3.

Oxygen molecules dissociated by the solar thermal and E-beam thermal and spectral combined are collected by a conceptual device called the Bessel Tube [25] that generates a drift axis under a cylindrical harmonic field where oxygen molecules are attracted and induced into the flow of oxygen molecules through the drift axis. Oxygen molecules that flow through the Bessel Tube are further sucked in by the turbo-molecular pump (TMP) for storage.

By increasing temperature of the regolith, the dissociation energy requirement of any chemical compound is reduced as shown in Figure 4 [6]. The correlation of dissociation potential vs. temperature is shown for several oxides in Figure 4. The dissociation of oxides requires less energy when the temperature of oxides is high. The column on right-hand side of Figure 4 shows the dissociation potential required to break down oxides at a temperature of 1700K. Dissociation of the regolith requires far less energy when already heated by the solar concentrator. The E-beam system provides the balance of energy required for dissociation. The lower the energy required to complete dissociation, then the higher the rate of dissociation by the E-beam system.

Assuming that lunar regolith when showered with electrons from an E-beam gun behaves like aluminum showered with beta particles, shown in Table 4, a setting of 60 keV would penetrate aluminum up to a depth of 0.097 mm. Further, among the oxides in regolith, the key breakdown potential to be considered is silica (7.33 eV) which is a majority among oxides in regolith. The numbers listed in Table 5 reflect the bonding energy of chemical mono-chains at the standard conditions. Alumina (Al_2O_3) like multi-chain chemicals requires much higher dissociation potentials as compared to those mono-chain chemicals. Another factor to be considered for the breakdown process is the temperature. When the temperature of chemicals is increased, the bonding energy is relaxed by the gained enthalpy, so that the energy required for dissociation is reduced. Figure 4 shows the effect of temperature on dissociation potentials. For example, the dissociation potential of silica at 1700 K drops to 1.51 eV. Accordingly, the combination of solar energy and E-beam energy offers better performance in dissociation.

Results

Using assumptions for penetration depths and chemical bonding energy for lunar regolith just discussed, projections for oxygen and metal production were calculated for two different size solar concentrators (5-meter diameter and 10-meter diameter) for three cases of E-beam guns: no E-beam guns added, two 15 kW E-beam guns added, and four 15 kW E-beam guns added.

Table 6 shows the oxygen production capabilities estimated with solar thermal, E-beam thermal + solar thermal, or E-beam spectral with the 5-meter and 10-meter Cassegrain systems. The 5-meter and 10-meter Cassegrain systems can collect and concentrate solar power with 80% efficiency after considering the reflectivity losses of Cassegrain reflectors and beam steering optics. Thus, solar thermal by the 5-meter Cassegrain amounts to be 21 kW level at the target area of regolith. With this solar power, the time required to melt the regolith of 0.25 kg by raising the temperature to 2000 K is determined by

$$\Delta t = \frac{m \cdot c_p \cdot \Delta T}{q_s} = \frac{0.25\,kg \cdot 2.9 \frac{kJ}{kgK} \cdot 2000K}{21 \frac{kJ}{s}} = 69\,\text{sec}\,onds$$

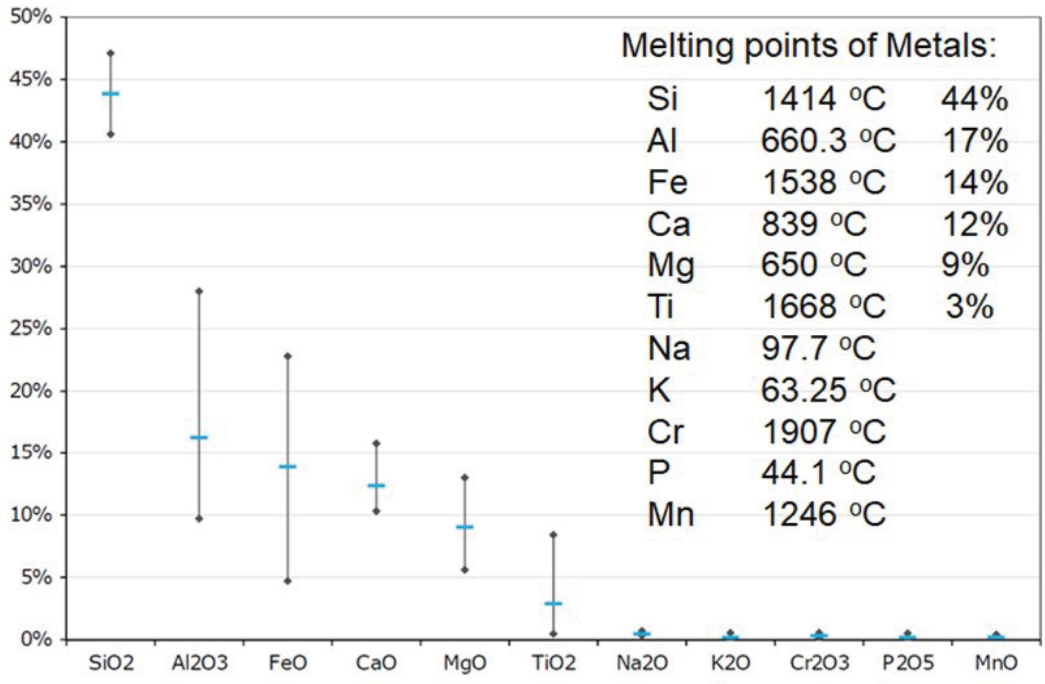

Figure 5: Abundance of oxides and melting points of metals, adapted from McKay, et al. [29].

Table 4: Beta particle maximum penetration depths [26].

Absorber	**Density (g/cm³)**	**Penetration Depth, mm**			
		2.3 MeV	**1.1 MeV**	**0.546 MeV**	**0.060 MeV**
Air	1.2 mg/cm³	8.8 m	3.8 m	1.9 m	0.23 m
Water (soft tissue)	1.10 g/cm³	11 mm	4.6 mm	2.28 mm	0.20 mm
Plastic (Acrylic)	1.2	9.6	4.0	1.99	0.197
Glass (Pyrex)	2.2	5.6	2.2	1.09	0.107
Aluminum	2.7	4.2	2.0	0.99	0.097
Gadolinium	7.9	1.7	0.7	0.35	0.034
Dysprosium	8.54	1.3	0.6	0.30	0.029
Copper	8.9	1.2	0.5	0.25	0.024
Lead	11.3	1.0	0.4	0.20	0.005

Table 5: Chemical bonding energy [27].

Single & Multiple Bonds	**Bonding Energy (kJ/mol)**	**Bonding Energy (eV)**	**Bond Length (pm)**
C-H	413	**4.29**	109
C-O	358	**3.72**	143
C=O	745	**7.74**	123
N-H	391	**4.06**	101
N-O	201	**4.35**	144
O-H	467	**4.85**	96
O-O	204	**2.12**	148
O-O (O_2)	498	**5.17**	121
Si-O	368	**3.83**	161
Al-O	102	**1.06**	17

1 eV ⊐ 96.49 kJ/mol; Bonding Energy: Energy needed to breakdown

Table 6: Oxygen production rates by solar thermal, solar + E-beam thermal, and E-beam spectral, based on current assumptions, 5-m and 10-m Cassegrain dishes.

Oxygen Production Rate				
	5-meter dish solar thermal (ST): 21 KW ($\dot{m}_{o2}$ = 65.8 grams for every 69 seconds)		**10-meter dish solar thermal (ST): 85 KW ($\dot{m}_{o2}$ = 131.7 grams for every 34 seconds)**	
Method	**Thermal (tons/yr)**	**Spectral (tons/yr)**	**Thermal (tons/yr)**	**Spectral (tons/yr)**
Solar Thermal + Spectral	28.299		114.543	
E-beam - 4 units (60 kV, 250 mA)	80.854	122.369	80.854	122.369
Solar + 4 E-beams	**109.153**	**150.668**	**195.397**	**236.912**
E-beam - 2 units (30 kV, 250 mA)	40.427	61.185	40.427	61.185
Solar + 2 E-beams	**68.726**	**89.484**	**154.97**	**175.728**

The specific heat (2.9 kJ/kgK) of regolith used in the equation above was obtained by the estimation using the 4th order polynomial at 1273 K [28]. Although the temperature in the above equation was 2000 K, the specific heat considered in the estimation was estimated using the median temperature 1273 K under the assumption that the regolith fed in is heated from the ambient temperature. In a similar way using 10-meter Cassegrain system of 85 kW solar power, the time required to melt 0.5 kg mass of regolith is estimated to be 34 seconds.

As summarized in Table 6, the extractable oxygen amount from 250 grams of regolith is 65.8 grams by 5-meter dish solar thermal for 69 seconds and 131.7 grams by 10-meter dish solar thermal for 34 seconds.

The oxygen production rate by solar thermal is 28.299 tons/year by the 5-meter solar concentrator and 114.543 tons/year by the 10-meter solar concentrator as tabulated in Table 6. The 5-meter solar concentrator is designed to process 250 grams of regolith with 21 kW solar power while 10-meter to process 500 grams of regolith. When E-beam thermal from the 4 units of 250 mA at 60 keV is added to solar thermal, the production rate of metals becomes 109.153 tons/year. The E-beam spectral alone adds 122.369 tons/year in the rate. The added effect when both E-beam spectral and solar thermal run together appears to be 150.668 tons/year. Table 7 tabulates the E-spectral cases for 30 keV and 60 keV of 250 mA beamline. In Table 7, the dissociation energy in J/g (the 5th column) is obtained from the dissociation energy in kJ/mol (the 3rd column) by multiplying 1000 and dividing by the molar weight of each oxide. Then, by dividing the E-beam power by the dissociation energy in J/g (the 5th column), the dissociation rates (the 6th column) are obtained for each oxide. The numbers in the 7th column reflect the percentage-based dissociation rate. For example, the percentage-based dissociation rate of SiO_2 case is obtained by multiplying 45.5% to the 6th column. The beamline of 250 mA carries 1.561×10^{18} electrons with the kinetic energy of 30 keV or 60 keV in this study cases. These kinetic energies of 30 keV and 60 keV are exceedingly higher than the dissociation energy listed in the 4th column. That's why the impinging energetic electrons on regolith split the oxides on the surface just like ablation or stripping action. This process itself only dissipates electron energy for splitting oxide molecules. So no lost process!! The initial carrying energy of electrons is used to split oxides, then the rest of energy of electrons undergoes the secondary or tertiary interactions continuously. The last column of Table 7 shows the results of oxide molecules coupled with energetic electrons after going through the primary, secondary, and tertiary interactions. Otherwise, oxygen and metal atoms split from oxides carry the rest of electron energy that might contribute to thermal energy. The results of coupled oxide molecules indicate the dissociation rate of each oxide.

$$\dot{m} = \frac{N_s \cdot M_o \cdot \Delta t}{N_A}$$

Where N_s is the number of molecules coupled with energetic electrons (the 13th column of Table 7), M_o the molar mass, Δt the processing time for production, and N_A the Avogadro number.

The addition of the E-beam system constitutes a 5-fold increase over solar thermal in oxygen production. Even when E-beam thermal is only considered, the production rates are nearly tripled.

Based on the results listed in Table 7, the production rates of oxygen and metals from regolith were estimated for the cases of 250 mA beamline of 30 keV and 60 keV. Table 8 shows the estimated production rates of oxygen and metals from regolith for the respective E-beam thermal and spectral cases.

The estimation of production rates that are listed in Table 8 includes not only everyone of oxides, but also anorthite ($CaAl_2Si_2O_8$) which has a combined composition of two SiO_2, Al_2O_3, and CaO. Interestingly, the dissociation rate of anorthite by E-beam appears to be better by average 20% as compared to the case of $2SiO_2+Al_2O_3+CaO$ which has the same 278 molar mass of anorthite. E-beam spectral, as opposed to E-beam thermal, is regarded as an instantaneous process for dissociation. Although the time constant of E-beam spectral is not estimated here, the overall time to break down oxides or anorthite is shorter than the time constant of thermal process. Even under the same power of E-beam, E-beam spectral outperforms the E-beam thermal for dissociation

Table 7: E-beam spectral estimations for both 30 keV and 60 keV of 250 mA beamline.

Oxides	Oxide in regolith	Dissociation Energy			Dissociation Rate							
					E-beam (250 mA, 30 KeV)		E-beam Spectral					
	%	kJ/mol	eV	J/g	g/s	%-base g/s	Ne, 250 mA	eV Ratio	Primary, N_1, # of oxide molecules/s	Seconary, N_2, # of oxide molecules/s	Tertiary, N_3, # of oxide molecules/s	Total, N_s, # of oxide molecules/s
SiO_2	45.5	707.6	7.33	11793	0.636	0.289	1.561E+18	4091	2.905E+21	1.07E+21	3.93E+20	4.37E+21
Al_2O_3	22.2	1030	10.67	100978	0.743	0.165	1.561E+18	2810	9.736E+20	3.58E+20	1.32E+20	1.46E+21
FeO	7.5	410.3	4.25	5699	1.316	0.099	1.561E+18	7055	8.257E+20	3.04E+20	1.12E+20	1.24E+21
CaO	15	431.3	4.47	7702	0.974	0.146	1.561E+18	6712	1.571E+21	5.78E+20	2.13E+20	2.36E+21
MgO	7.8	418.7	4.34	10468	0.717	0.056	1.561E+18	6914	8.415E+20	3.10E+20	1.14E+20	1.27E+21
TiO_2	1.3	669.9	6.94	8374	0.896	0.012	1.561E+18	4321	8.766E+19	3.23E+19	1.19E+19	1.32E+20
Oxides	**Oxide in regolith**	**Dissociation Energy**			**Dissociation Rate**							
					E-beam (250 mA, 60 KeV)		**E-beam Spectral**					
	%	**kJ/mol**	**eV**	**J/g**	**g/s**	**%-base g/s**	**Ne, 250 mA**	**eV Ratio**	**Primary, N_1, # of oxide molecules/s**	**Seconary, N_2, # of oxide molecules/s**	**Tertiary, N_3, # of oxide molecules/s**	**Total, N_s, # of oxide molecules/s**
SiO_2	45.5	707.6	7.33	11793	1.272	0.579	1.561E+18	8182	5.809E+21	2.14E+21	7.86E+20	8.73E+21
Al_2O_3	22.2	1030	10.67	100978	1.485	0.330	1.561E+18	5621	1.947E+21	7.16E+20	2.64E+20	2.93E+21
FeO	7.5	410.3	4.25	5699	2.635	0.197	1.561E+18	14110	1.651E+21	6.08E+20	2.24E+20	2.48E+21
CaO	15	431.3	4.47	7702	1.948	0.292	1.561E+18	13423	3.142E+21	1.16E+21	4.25E+20	4.72E+21
MgO	7.8	418.7	4.34	10468	1.433	0.112	1.561E+18	13827	1.683E+21	6.19E+20	2.28E+20	2.53E+21
TiO_2	1.3	669.9	6.94	8374	1.791	0.023	1.561E+18	8642	1.753E+20	6.45E+19	2.37E+19	2.64E+20

Table 9: Metal production rates by solar thermal, solar + E-beam thermal, and E-beam spectral, based on current assumptions, 5-m dish and 10-m Cassegrain dish.

Metal Production Rate				
	5-meter dish solar thermal (ST): 21 KW ($\dot{m}_M$ = *84 grams for every 69 seconds*)		**10-meter dish solar thermal (ST): 85 KW ($\dot{m}_M$ = *168 grams for every 34 seconds*)**	
Method	**Thermal (tons/yr)**	**Spectral (tons/yr)**	**Thermal (tons/yr)**	**Spectral (tons/yr)**
Solar Thermal + Spectral	39.388		159.428	
E-beam - 4 units (60 kV, 250 mA)	112.538	168.402	112.538	168.402
Solar + 4 E-beams	**151.926**	**207.790**	**271.966**	**327.830**
E-beam - 2 units (30 kV, 250 mA)	28.135	42.101	28.135	42.101
Solar + 2 E-beams	**67.523**	**81.489**	**187.563**	**201.529**

Table 8: Oxygen and metal production rates by E-beam for both thermal and spectral

Oxides	**Oxide in regolith**	**E-beam: 250 mA, 30 KeV**				**E-beam: 250 mA, 60 KeV**			
	%	**E-beam Thermal**		**E-beam Spectral**		**E-beam Thermal**		**E-beam Spectral**	
		O_2 (tons/y)	**Metal (tons/y)**	**O_2 (tons/y)**	**Metal (tons/y)**	**O_2 (tons/y)**	**Metal (tons/y)**	**O_2 (tons/y)**	**Metal (tons/y)**
SiO_2	45.5	4.836	4.289	7.317	6.403	9.673	8.578	14.635	12.805
Al_2O_3	22.2	2.444	2.756	3.679	4.139	4.888	5.512	7.358	8.278
FeO	7.5	0.685	2.428	1.040	3.640	1.370	4.856	2.080	7.280
CaO	15	1.290	3.317	1.979	4.947	2.580	6.633	3.958	9.894
MgO	7.8	0.750	1.057	1.060	1.590	1.410	2.115	2.120	3.180
TiO_2	1.3	0.147	0.220	0.221	0.331	0.294	0.441	0.442	0.662
Total		10.107	14.067	15.296	21.050	20.213	28.134	30.592	42.100
$2SiO_2 + Al_2O_3 + CaO$	82.7	13.406	14.651	20.292	21.892	29.181	29.301	40.586	43.784
Anorthite $CaAl_2Si_2O_8$	60 [17]	15.592	18.272	23.443	27.472	31.184	36.544	46.886	54.945
Difference		2.186	3.621	3.151	5.580	2.003	7.243	6.300	11.161
% Difference		16%	25%	15.5%	25.5%	7%	25%	15.5%	25.5%
2 E-beam Guns	Total	20.213	28.134	30.592	42.100	40.427	56.269	61.185	84.201
	Anorthite	31.184	36.544	46.886	54.944	62.368	73.088	93.772	109.890
4 E-beam Guns	Total	40.427	56.269	61.185	84.201	80.854	112.538	122.369	168.402
	Anorthite	62.368	73.088	93.772	109.888	124.736	146.176	187.544	219.780

of oxides or anorthite. Even though this analysis does not cover ilmenite because of insufficient data, it is obvious that a similar nature of conclusion can be extended over ilmenite.

Table 9 shows the metal production capability by solar thermal, E-beam thermal + solar thermal, or E-beam spectral with the 10-meter Cassegrain system. The metal production rate by solar thermal is 39.388 tons/year with the 5-meter Cassegrain system and 159.428 tons/year with the 10-meter Cassegrain system. For the case of 5-meter Cassegrain, when E-beam thermal with 4 units of 250 mA at 60 keV is added to solar thermal, the production rate of metals becomes 112.538 tons/year. The E-beam spectral alone adds 168.402 tons/year in rate.

For the 10-meter Cassegrain system with four E-beam lines of 250 mA at 60 keV, the solar thermal plus E-beam thermal enables 271.966 tons/year metal production. With E-beam spectral, it can produce 327.830 tons/year of metal. The added effect of both E-beam spectral and thermal is hard to count because the energy distribution of energetic electrons after the primary interaction is not apparently known, except the energy carried by the split parts of oxide molecules is thermal and the penetration of energetic electrons into oxide is decayed exponentially, almost following the rule of Beer-Lambert law. The addition of the E-beam system constitutes nearly a 5-fold increase in metal production when the 5-meter solar thermal considered. Even when E-beam thermal is only considered, the production rates are more than doubled.

Based on the production rates of metals determined by the solar thermal, the E-beam spectral, or the Solar thermal + E-beam thermal, when a 10-kW induction crucible is used

to sort and separate metals, the metal processing time for the 5-meter and 10-meter Cassegrain systems takes approximately 10 seconds for 0.25 kg and 20 seconds for 0.5 kg, respectively. Table 10 lists the oxygen and metal production rate, required energy to melt, and times. It lists somewhat detailed metal production rates from oxides when E-beam spectral is considered, and the energy and times required for sorting out the species of metal by the inductive heating method. Induction heating offers a capability of heating rate control by modulating the applied frequency and current to sort and separate metals according to their melting temperatures. The numbers in the pink and blue shaded areas indicate metal production rates when E-beam spectral was added to the solar thermal process using the 10-meter and 5-meter Cassegrain systems.

Specifically, the described system offers a new approach for mineral separation and processing of 1) High-titanium mare/ilmenite for titanium extraction and separation, and 2) Sources of KREEP (potassium, rare Earth elements, and phosphorus) for extraction and separation of rare Earth elements without the need for reactants or valves for passing abrasive granular material.

Discussion

The results from analysis illustrate the scalability and increased production rates when adding energetic E-beam energy to the oxygen and metal extraction system concept. Production rates of oxygen and metals from regolith by the E-beam energy are comparable to the production rates possible when using only solar thermal, as shown in Table 6 and Table 9. Accordingly, when combined, the solar thermal and E-beam offer enhanced production rate of oxygen and metals. However, as described above and illustrated by Figure 4, the purpose for adding the e-beam gun is to separate the oxygen from the regolith while the metals remain in solid form. Specifically, the key merits of use of the E-beam

Table 10: Production rates of metals in lunar regolith.

Metal Oxides in Regolith	Metal	T_M (°C)	Oxide (%)	C_p, (J/g °C)	Oxide Mass		500 g regolith batch - 10m		250g regolith batch - 5m		Energy to melt metal, KJ		Time to melt by KW, sec	
					500 g batch	250 g batch	M_{metal} (ton/y)	O_2 (ton/y)	M_{metal} (ton/y)	O_2 (ton/y)	500 g	250 g		
SiO_2	Si	1414	45.5%	0.7	227.5	113.7	100	113	38	43	101	50.5	10	5
							74	84	25	28				
Al_2O_3	Al	660.3	22.2%	0.9	111	55.5	64	57	24	22	27	13.5	2.7	1.4
							48	42	15	14				
FeO	Fe	1538	7.5%	0.442	37.5	18.75	57	16	21	6	37	18.5	3.7	1.9
							42	12	14	4				
CaO	Ca	839	15%	0.15	75	37.5	77	30	29	12	5.5	2.7	0.6	0.3
							57	23	19	8				
MgO	Mg	650	7.8%	1.017	39	19.5	25	16	9	6	18	9	1.8	0.9
							18	12	6	4				
TiO_2	Ti	1668	1.3%	0.544	6.5	3.25	5	3.4	2	1	8.5	4.2	0.9	0.5
							4	2.5	1	1				
Na_2O	Na	97.7	< 1%	1.214	1	0.5		0.26		0.13	1	0.5	0.1	0.05
K_2O	K	63.25	< 1%	0.753	1	0.5		0.17		0.09	0.5	0.2	0.05	0.02
Cr_2O_3	Cr	1907	< 1%	0.460	1	0.5		0.32		0.17	left	left		
P_2O_5	P	44.1	< 1%	0.8	1	0.5		0.56		0.28	0.1	0.05	0.01	0.01
MnO	Mn	1246	< 1%	0.477	1	0.5		0.23		0.12	5	2.5	0.5	0.25

E-beam energy (4 units: 60 kW) added

E-beam energy (2 units: 60 kW) added

E-beam energy (4 units: 30 kW) added

E-beam energy (2 units: 30 kW) added

system for the breakdown of regolith for oxygen and metal productions are owed to the facts that the E-beam system operates at lunar high vacuum and the coupling efficiency of E-beam is regarded very high because energetic electrons can penetrate deep into material as shown in Figure 2. The penetrated energetic electrons are known to have secondary and tertiary interactions. For example, energetic electrons in primary interaction immediately dissociate oxide molecules which have bonding energy less than 10 eV as listed in Table 3, Table 5 and Table 7. After the primary interaction, the electron carrying the rest of energy undergoes the secondary interaction and likewise the tertiary interaction too. In such a manner, energetic electrons have a more effective role of decomposition of regolith than solar. In the primary interaction, a number of energetic electrons (1.5625×10^{18} for 250 mA beamline) that impinge on oxides of regolith can dissociate approximately the same number of oxide molecules and remove the oxygen and metal atoms from the surface where the interaction took place. The products from dissociation fly away from the surface without staying on because of the process in high vacuum. Then, the beamline consecutively interacts with and strips the next surface layer of oxides, just like shaving the surface. This kind of E-beam processing can be found in the E-beam machining that leaves no burrs and residues while in machining process. When those oxides are heated to a high temperature, the bonding energy of oxides is reduced as shown in Figure 4. The reduction in bonding energy by raising temperature does not require much energy. On the other hand, it can be interpreted as increased production of oxygen and metals if the system adds the power of E-beam as listed in Table 6, Table 7, Table 9, and Table 10. The results of this case study encourage a combined system of solar thermal to work with E-beam together. These estimated projections are based on assumptions that have not been validated by laboratory tests with E-beam guns at these power levels.

Specifically, the described system offers a new approach for oxygen and mineral separation and processing from lunar regolith. Given the promising theoretical analysis presented herein, there are other benefits anticipated by our current understanding of E-beam systems operating at these power levels. Although our analysis shows substantial advantage for operating the E-beam and solar thermal systems together, if necessary, the E-beam system does not require sunlight to operate.

When E-beam that carries sufficient energy scans over any materials, the energy of E-beam breaks the bonding structure of material into atoms and molecules, and eventually the ablated atoms and molecules are blown away since E-beam operates in a vacuum environment. Breakdown of bonding structure by E-beam spectra that leads dissociation is not thermal process, but instantaneously disconnect any bonding structures chemically tied up with ionic or covalent or dangling bond. This instantaneous action has been observed by others [30]. Accordingly, the process time is fast as opposed to long time-constant of thermal process. This aspect of E-beam spectral explains why the processing time of E-beam spectral is short or on the other hand, the production rate of oxygen and metals is better than E-beam thermal as listed in Table 8. Another aspect of E-beam spectral explains that for the case when the viscosity of a molten surface traps oxygen bubbles, the E-beam spectral can ablate the trapping layer while dissociating oxides and free the trapped oxygen bubbles. Furthermore, the E-beam spectral decomposes oxide mostly without heating or melting the regolith. Additionally, the E-beam spectral requires less power to liberate oxygen when regolith is at higher temperatures, as shown in the right-hand side of Figure 4.

With an understanding of the relative production rates among solar thermal, E-beam spectral, and E-beam thermal, we can provide an example of how these three processes would be applied for separating the oxygen and metals from lunar regolith. As an example, anorthite ($CaAl_2Si_2O_8$) has a combined composition of two SiO_2, Al_2O_3, and CaO. Shown in Figure 5, Al, Ca, and Si have melting points of 660.3 °C, 839 °C, and 1414 °C, respectively. Our approach is to implement a stepwise process that raises the temperature to specific values and applies E-beam spectral to separate the oxygen and the metals. For anorthite, the first temperature to reach and hold corresponds to Al. While the regolith temperature is held just below 660 °C, the E-beam spectral will assist in liberating the oxygen. The temperature is then raised to melt the Al away. One option is to vaporize the Al and extract it from the chamber before proceeding to the next metal.

Another fundamental feature that favors the E-beam approach is that solar thermal losses occur when the sunlight is reflected by the melted shining surface of regolith rather than fully absorbed. Also, there is the potential for some transmission losses as sunlight passes through the optics. In our analysis, we accounted for 20% losses in the production rates shown above. However, for e-beam at 250 mA, the electrons at kinetic energies of 30 keV and 60 keV experience no reflection at the melted shining surface of regolith. Furthermore, the efficiency of E-beam systems is typically around 90-95%. The combined system is powered by sunlight available on the lunar southpole. Therefore, the combined E-beam and solar thermal system offers a high-efficiency, high-ISRU approach to oxygen and metals extraction while requiring no expensive supply chains and taking advantage of the natural vacuum pressure conditions on the lunar surface.

The system concept (see Figure 3) provides for the collection of oxygen and other gases as they are produced so that they do not recombine with the regolith. That technology is known as a Bessel Tube for Lunar Volatiles Collection [25]. As mentioned in the literature, vapor pyrolysis can be used for extracting metals and minerals from the regolith. Additionally, our system concept provides for metal separation through an induction heating process using an induction crucible concept. Like vapor pyrolysis, our system depends on sunlight. Unlike other approaches involving molten regolith, we attempt to avoid handling molten material by heating the regolith so that the e-beam uses as little power necessary to complete the oxygen removal from the regolith while also leaving in solid form, the metals to fall towards the collection crucibles.

Conclusions

Theoretical analysis was performed to demonstrate the

dissociation capability of oxide molecules in lunar regolith by the energetic E-beam in combination with solar thermal. As illustrated in Tables 5, 7, 8, 9, 10. The oxygen and metal production rates by solar thermal, E-beam spectral, E-beam thermal, or combination of these were estimated. Most oxides have a bonding energy less than 7 eV. Once these oxides are thermalized by increasing temperature, the bonding energy of oxides is reduced as shown in Figure 4. Accordingly, the combination of solar thermal, E-beam spectral, and E-beam thermal offers a great advantage to increase the production rates of oxygen and metals from lunar regolith up to 7-fold. Although solar spectral carries deep UV, the benefits by its own low energy and poor penetration depth are not comparable to energetic E-beam spectral. Experimental study is necessary for the verification of performance enhancement on oxygen and metal production rates by E-beam spectral and thermal.

References

1. (2023) NASA Invites Stakeholders to STMD's LIFT-1 Industry Forum.
2. (2023) Request for Information: Lunar Infrastructure Foundational Technologies-1 (LIFT-1) Demonstration.
3. NASA ISRU Envisioned Future Priorities. Strategic Framework, Charting the horizon of NASA technology development.
4. (2023) NASA's Moon to Mars Strategy and Objectives Development: A blueprint for sustained human presence and exploration throughout the Solar System.
5. Pirtie Z, McBrayer K, Beauchemin A (2023) Artemis, Ethics and Society: Synthesis from a Workshop.
6. Schluter L, Cowley A (2020) Review of techniques for in-situ oxygen extraction on the moon. Planetary and Space Science 181: 104753.
7. Rasera JN, Cilliers JJ, Lamamy JA, et al. (2020) The beneficiation of lunar regolith for space resource utilisation: A review. Planet Space Sci 186: 104879.
8. Schwandt C, Hamilton JA, Fray DJ, et al. (2012) The production of oxygen and metal from lunar regolith. Planet Space Sci 74: 49-56.
9. Shaw MG, Humbert M, Brooks G, et al. (2022) Mineral processing and metal extraction on the lunar surface - Challenges and Opportunities. Mineral Processing and Extractive Metallurgy Review 43: 865-891.
10. Agosto WN (1985) Electrostatic concentration of lunar soil minerals. Lunar Bases and Space Activities of the 21st Century 453.
11. Kim K, Elsayed-Ali HE (1982) Investigation of electron-beam charging for inertial-confinement-fusion targets. Charged Particle Research Laboratory Report No. 3-82.
12. Wang X, Schwan J, Hsu HW, et al. (2016) Dust charging and transport on airless planetary bodies. Geophys Res Lett 43: 6103-6110.
13. Chelsea G (2021) Arcs of 'lightning' on the moon could be the future of lunar mining. Space.com.
14. Yang W, Sun Q, Zhou Q (2020) Particle modeling of vacuum arc discharges. J Appl Phys 128: 060905.
15. Choi S, Moses R, Park C, et al. (2020) Implementation concept of operations for a multi-purpose cassegrain solar concentrator, micro-spectrometers, and electrostatic neutralizers to enable in situ construction activities plus lunar, planetary, and deep space science exploration on the moon. NASA Technical Report.
16. Turkevich AL (1973) The average chemical composition of the lunar surface. Proceedings of the Lunar Science Conference 4: 1159-1168.
17. McKay DS, Williams RJ. A geologic assessment of potential lunar ores. V-4.
18. Cremonese G, Borin P, A Lucchetti, et al. (2013) Micrometeoroids flux on the Moon. Astronomy & Astrophysics 551.
19. Ptacek P, Opravil T, Šoukal F, et al. (2013) Kinetics and mechanism of formation of gehlenite, Al–Si spinel and anorthite from the mixture of kaolinite and calcite. Solid State Sciences 26: 53-58.
20. Brewer L (1953) The thermodynamic properties of the oxides and their vaporization processes. Chemical Reviews 52: 1-75.
21. David L (2005) CRC standard thermodynamic properties of chemical substances. The Handbook of Chemistry and Physics. (85th edn), CRC Press.
22. Lamboley K (2022) System architecture for lunar oxygen production from regolith using a model-based system engineering approach. Degree Project in Vehicle Engineering, Second Cycle, 30 Credits Stockholm, Sweden.
23. Matchett J (2006) Production of lunar oxygen through vacuum pyrolysis. The George Washington University.
24. https://courses.physics.illinois.edu/npre441/sp2021/course%20materails/chapter2%20part%201%20interaction%20of%20beta%20particles.pdf
25. Choi SH, Moses RW (2022) Lunar Volatiles Collector (LVC). ARC.
26. Wang Y (1969) CRC Handbook of Radioactive Nuclides. Chemical Rubber Company, Ohio.
27. Silberberg M (2021) The molecular nature of matter and changes. (9th edn), McGraw-Hill.
28. Woods-Robinson R, Siegler MA, Paige DA (2019) A model for the thermophysical properties of lunar regolith at low temperatures. JGR Planets 124: 1989-2011.
29. McKay DS, Heiken GH, Basu A, et al. (1991) The lunar regolith. In: Heiken G, Vaniman D, French BM, The lunar sourcebook. Cambridge University Press, Cambridge, Massachussetts, 285-356.
30. Daniel A, Irmgard F (2002) Breaking bonds by mechanical stress: When do electrons decide for the other side? J Am Chem Soc 124: 3402-3406.

DOI: 10.36959/422/469